Radiation Measurements 150 (2022) 106692

Contents lists available at ScienceDirect

Radiation Measurements

journal homepage: www.elsevier.com/locate/radmeas

On the various-heating-rates method for evaluating the activation energies of thermoluminescence peaks

R. Chen [a,*], J.L. Lawless [b], V. Pagonis [c]

[a] Raymond and Beverly Sackler School of Physics and Astronomy, Tel Aviv University, Tel Aviv, 69978, Israel
[b] Redwood Scientific Incorporated, Pacifica, CA94044-4300, USA
[c] Physics Department, McDaniel College, Westminster, MD21157, USA

ARTICLE INFO

Keywords:
TL
Various heating rates
OTOR model

ABSTRACT

The well-known various-heating-rates (VHR) method for evaluating the activation energy of thermoluminescence (TL) peaks is revisited. The method hinges on the shift of the TL peak with changing heating rate, and is based on the properties of first-order curves. Several works have shown that the same method yields a good approximation of the activation energy when general-order peaks are involved. A recent work by Maghrabi has presented a heuristic explicit expression for the magnitude of the shift between two heating rates within the first-order kinetics framework. In the present work, we address two related points. We show how the expression suggested by Maghrabi can be reached by making a very reasonable approximation of the original equation yielding the maximum condition. We also present an alternative expression which yields the amount of shift of the TL maximum with changing heating rate and with less approximation. The other point dealt with involves the results of a numerical study of the evaluation of the activation energy by the use of various heating rates in the more general one-trap-one-recombination-center (OTOR) situation. The results show that even in this general case, the various heating rates method yields very good results. The same is true for the "mixed-order" kinetics. The numerical results are accompanied by an analytical account which shows that the method yields very accurate activation energies in the rather general OTOR situation.

1. Introduction

The method of various heating rates for evaluating the activation energy of a thermoluminescence (TL) glow peak is based on the well-known expression of first-order kinetics introduced by Randall and Wilkins (1945). Very briefly, the first-order equation governing the process is

$$I(T) = -dn/dt = sn\exp(-E/kT), \tag{1}$$

where n (cm^{-3}) is the instantaneous occupancy of the relevant trap, E (eV) the activation energy, s (s^{-1}) the frequency factor, k (eV/K) Boltzmann's constant, T (K) the temperature, t (s) time and $I(T)$ the TL intensity. When a linear heating function $T = T_0 + \beta t$ is used and where T_0 (K) is the initial temperature and β (K/s) the constant heating rate, the TL expression $I(T)$ can be written explicitly as

$$I(T) = sn_0\exp(-E/kT)\exp\left[-(s/\beta)\int_{T_0}^{T}\exp(-E/kT')dT'\right], \tag{2}$$

where n_0 (cm^{-3}) is the initial concentration of trapped carriers and T' is an integration variable. This curve is a peak-shaped asymmetric curve with the fall-off side significantly narrower than the low-temperature side. By equating the derivative to zero, one gets the maximum condition

$$\beta E/\left(kT_m^2\right) = s\exp(-E/kT_m), \tag{3}$$

where T_m (K) is the temperature at the maximum. For a certain TL peak, when the heating rate increases, the maximum temperature also increases. This can be easily shown by re-writing Eq. (3) as

$$\beta = (sk/E)T_m^2\exp(-E/kT_m). \tag{4}$$

Increasing the heating rate β must increase the right-hand side by the

* Corresponding author.
E-mail address: chenr@tauex.tau.ac.il (R. Chen).

https://doi.org/10.1016/j.radmeas.2021.106692
Received 6 October 2021; Received in revised form 1 December 2021; Accepted 3 December 2021
Available online 8 December 2021

same amount, but since $T_m^2\exp(-E/kT_m)$ is an increasing function of T_m, increasing β must result in an increase in T_m. It should be noted that Osada (1960) has shown that the same equations, (3, 4) take place when the heating rate is exponential provided that β is replaced by β_m, the instantaneous heating rate at the maximum. Chen and Winer (1970) have later proven that the same equations are valid for any monotonically increasing heating function when, again, the instantaneous heating rate at the maximum, β_m is used in Eqs. (3) and (4). Of course, this is exactly true for first-order kinetics. Three works published independently in the same year by Bohun (1954), Booth (1954) and Parfianovitch (1954) suggested a method for evaluating the activation energy from a first-order peak by repeating the measurement of a TL peak at two heating rates, β_1 and β_2. By writing Eq. (4) twice, for the two heating rates, dividing one by the other and rearranging, one gets

$$E = [kT_{m1}T_{m2} / (T_{m1} - T_{m2})]\ln\left[(\beta_1 / \beta_2)(T_{m2}/T_{m1})^2\right], \tag{5}$$

where T_{m1} and T_{m2} are the temperatures at the maximum with heating rates β_1 and β_2, respectively. An extension to this method has been given by Hoogenstraaten (1958) who suggested the use of several heating rates. A plot of $\ln(T_m^2/\beta)$ vs. $1/T_m$ would, according to Eq. (3), yield a straight line from whose slope E/k, the activation energy E is readily found. The intercept of the straight line with the y-axis gives the value of $\ln(sk/E)$ from which the frequency factor s can be determined.

Garlick and Gibson (1948) showed that under circumstances of relatively strong retrapping of thermally released carriers second-order kinetics may result, yielding the kinetic equation

$$I(T) = -dn/dt = s' n^2 \exp(-E/kT), \tag{6}$$

where s' is the pre-exponential factor ($\mathrm{cm^3 s^{-1}}$). The solution of this equation yields a nearly symmetric curve. May and Partridge (1964), in an attempt to deal with cases with symmetries intermediate between that of first order and second order, used the "general order" equation

$$I(T) = -dn/dt = s' n^b \exp(-E/kT), \tag{7}$$

where $1 \le b \le 2$ and s', the pre-exponential factor, has dimensions of $\mathrm{cm^3}^{(b-1)}\mathrm{s^{-1}}$. It should be mentioned that excluding the case of $b = 1$ and $b = 2$, Eq. (7) is a heuristic approximation to a more complicated situation. It enables the presentation of intermediate-symmetry TL peaks, but it cannot be derived from the more realistic set of three simultaneous differential equations governing the one-trap-one-recombination-center (OTOR) case (see below). As for the method of various heating rates, Chen and Winer (1970) showed that although the VHR method was developed for the first-order case, it yields very good values for the general-order cases, including the second order where $b = 2$.

In the present work, we consider the following points. One has to do with an explicit expression for the shift of the maximum intensity when the heating rate is varied in the first-order case, which is also expected to be a very good approximation in the general-order situation as mentioned above. Another point checks the usability of the VHR method for peaks subject to the more physical OTOR model both by a numerical example and an analytical treatment. Two specific cases are also discussed, namely, the case of mixed-order kinetics and the model considering the TL in feldspars and their behavior under VHR measurements.

2. Explicit expressions for the shift of the TL maximum with heating rate

Following many publications dealing with the evaluation of the activation energy using two measurements at two heating rates, Maghrabi (2018) raised the point of evaluating the temperature of the maximum, T_{m2}, reached by a first-order peak with a heating rate of β_2, while the maximum of the same peak occurs at T_{m1} when a heating rate of β_1 is used. The empirical equation he gave was

$$T_{m2} = T_{m1}(\beta_2/\beta_1)^{kT_{m1}/E}. \tag{8}$$

Let us show how this approximation can be reached from Eq. (4). We would like to calculate $dT_m/d\beta$, but to begin with, it is easier to find the inverse, $d\beta/dT_m$. The derivative of Eq. (4) yields

$$\frac{d\beta}{dT_m} = \frac{sk}{E}\exp(-E/kT_m)(2T_m + E/k) = s\exp(-E/kT_m)\left(\frac{2kT_m}{E} + 1\right). \tag{9}$$

Substituting $s\cdot\exp(E/kT_m)$ from Eq. (3) and since always $2kT_m/E \ll 1$, we get

$$\frac{d\beta}{dT_m} = \frac{\beta E}{kT_m^2}\left(\frac{2kT_m}{E} + 1\right) \cong \frac{\beta E}{kT_m^2}. \tag{10}$$

Inverting this expression, using again the smallness of $2kT_m/E$ and considering again Eq. (3), we get

$$\frac{dT_m}{d\beta} \cong \frac{k}{E}\frac{T_m^2}{\beta} = s^{-1}\exp(E/kT_m). \tag{11}$$

Equation (11) shows again that $T_m(\beta)$ is an increasing function. However, since T_m varies very slowly with the heating rate, we can write the approximate equation

$$\frac{dT_m}{T_m} = \left(\frac{kT_m}{E}\right)\frac{d\beta}{\beta}, \tag{12}$$

where T_m is the maximum temperature with the heating rate β. Integrating from T_{m1} to T_{m2}, i.e. from β_1 to β_2 and assuming that T_m is a very weak function of β (see also Maghrabi (2018)), one gets

$$\ln(T_{m2}/T_{m1}) = \left(\frac{kT_{m1}}{E}\right)\ln(\beta_2/\beta_1). \tag{13}$$

Taking the exponential of both sides one gets

$$\frac{T_{m2}}{T_{m1}} = \left(\frac{\beta_2}{\beta_1}\right)^{kT_{m1}/E}, \tag{14}$$

or, by multiplying both sides by T_{m1} we get Eq. (8) previously reached empirically by Maghrabi (2018).

We can also present another explicit expression for the amount of shift, based on Eq. (11) which can be developed without further approximations. From Eq. (11), we can write

$$\frac{dT_m}{T_m^2} = \frac{k}{E}\frac{d\beta}{\beta}. \tag{15}$$

By integration we get immediately

$$\frac{1}{T_{m1}} - \frac{1}{T_{m2}} = \frac{k}{E}\ln\left(\frac{\beta_2}{\beta_1}\right), \tag{16}$$

and by rearranging we get the explicit expression

$$T_{m2} = \frac{T_{m1}}{1 - \frac{kT_{m1}}{E}\ln(\beta_2/\beta_1)} = \frac{T_{m1}}{1 - \ln(\beta_2/\beta_1)^{kT_{m1}/E}}. \tag{17}$$

Equation (17) is more complicated than Eq. (8), but somewhat more accurate. The connection between these two equations can be realized by noting that since $kT_{m1}/E \ll 1$, we have $\ln(\beta_2/\beta_1)^{kT_{m1}/E} \simeq 1$ and therefore

$$T_{m2} \approx T_{m1}\left[1 + \ln(\beta_2/\beta_1)^{kT_{m1}/E}\right] \approx T_{m1}(\beta_2/\beta_1)^{kT_{m1}/E}, \tag{18}$$

which is back to Eq. (8).

3. Numerical solution of the OTOR equations at various heating rates

As pointed out above, the first-order and second-order equations are

extreme cases of weak and strong retrapping respectively. The method of various heating rates was developed accurately for the former and was shown to yield very good approximate results for the latter as well as for the empirical "general-order" kinetics mentioned above. In the present section, we would like to check the shift of the maximum TL temperature and the evaluated E values reached by the VHR method in the more physical OTOR framework of three simultaneous differential equations governing the transitions between an electron trap, a hole center and the conduction band. The relevant equations are (see e.g. Halperin and Braner, 1960),

$$I(T) = -dm/dt = A_m m n_c, \tag{19}$$

$$dn/dt = A_n(N-n)n_c - sn\exp(-E/kT), \tag{20}$$

$$dn_c/dt = dm/dt - dn/dt. \tag{21}$$

Here, n (cm^{-3}) and m (cm^{-3}) are, respectively the instantaneous concentrations of electrons in traps and holes in centers. n_c (cm^{-3}) is the instantaneous concentration of electrons in the conduction band. N (cm^{-3}) is the concentration of traps. A_m (cm^3s^{-1}) and A_n (cm^3s^{-1}) are the recombination and retrapping probability coefficients, respectively. s (s^{-1}) is the frequency factor, E (eV) the activation energy, k ($eV{\cdot}K^{-1}$)-Boltzmann's constant and T (K) the absolute temperature. $I(T)$ is the intensity of emitted TL, given in units of $cm^{-3}s^{-1}$.

Following Randall-Wilkins and Garlick-Gibson, Halperin and Braner (1960) made the "usual" quasi-equilibrium assumption, namely

$$n_c << n; \quad |dn_c/dt| << |dn/dt|, \tag{22}$$

and reached the single equation in the two variables, n and m,

$$I(T) = -\frac{dn}{dt} = sn\exp(-E/kT)\frac{A_m m}{A_m m + A_n(N-n)}. \tag{23}$$

Kannunikov (1978) suggested that as long as only one trapping state and one kind of recombination center are involved, $n = m$ and therefore,

$$I(T) = -\frac{dn}{dt} = s\exp(-E/kT)\frac{A_m n^2}{A_m n + A_n(N-n)}, \tag{24}$$

which is a differential equation in one variable. We have solved numerically the set, Eqs. 19–21, for samples of sets of chosen parameters. We preferred to solve the equations without the additional quasi-equilibrium assumption since the solver is very efficient in performing this kind of solutions and the results are expected to be practically the same. If there is a difference, we note that Eqs. 19–21 are physically more valid than Eq. (24). We have used the Matlab solver ode15s and in each simulation, we assumed that $n_0 = m_0$ since the model includes a single trapping state and a single kind of recombination center. We used a linear heating function,

$$T = T_0 + \beta t, \tag{25}$$

where T_0 (K) is the initial temperature and β (K/s) is the constant heating rate. For each set of chosen parameters, the simulation was run twice, for two heating rates, 1K/s and 2K/s. The two maximum temperatures were recorded and the evaluated activation energy was determined by Eq. (5). The parameters chosen were $E = 1$ eV; $s = 10^{12}$ s^{-1}; $A_m = 10^{-8}$ cm^3s^{-1}; $N = 10^{14}$ cm^{-3}; $n_0 = m_0 = 10^{12}$ cm^{-3} and A_n was variable as shown in Table 1.

Table 1
Evaluated maximum temperatures and symmetry factors in simulated TL peaks with different values of the retrapping coefficient and the activation energies determined thereof. The other parameters are given in the text.

A_n (cm^3s^{-1})	T_{m1}/T_{m2} (K)	μ_{g1}/μ_{g2}	E_β (eV)
10^{-12}	384.577/393.038	0.4193/0.4194	1.00000
10^{-11}	384.992/393.470	0.4363/0.4366	1.00010
10^{-10}	391.650/400.411	0.4911/0.4914	1.00089
10^{-9}	414.320/424.091	0.5163/0.5167	1.00184
10^{-8}	447.365/458.710	0.5209/0.5213	1.00231

The table shows the values of the maximum temperature for different values of the retrapping probability coefficient A_n and the corresponding T_m values for $\beta = 1$ and 2 K/s, the values of the symmetry factors μ_g and the activation energies evaluated by the VHR method, Eq. (5). When A_n varies gradually from 10^{-12} to 10^{-8} cm^3s^{-1}, the symmetry factor indicates transition from effective first-to effective second-order kinetics, but the activation energy evaluated differs from the inserted value only by <0.25% all along.

4. Analytical approach

4.1. General one-trap one-center model

Following the numerical example, let us develop a broader analytical treatment of the various heating rates method in the OTOR model. Let us start with equation (24) along with the linear heating rate, Eq. (25). The usual variable plot shows β/T_m^2 on a log scale against $1/kT_m$. For first-order kinetics, the slope of this plot is -*E*,

$$\frac{d\ln(\beta/T_m^2)}{d(1/kT_m)} = -E. \tag{26}$$

For second-order kinetics or the more general one-trap-one-center (OTOR) kinetics, Eq. (26) is no longer true. Let us generalize Eq. (26) to

$$\frac{d\ln(\beta/T_m^2)}{d(1/kT_m)} = -C_f E, \tag{27}$$

where C_f is a correction factor to account for non-first-order kinetics.

To prepare for finding the maximum, we need the derivative of I (Eq. (24)),

$$\frac{dI}{dt} = \left[\frac{E\beta}{kT^2} + \left(\frac{2}{n} - \frac{A_m - A_n}{A_m n + A_n(N-n)}\right)\frac{dn}{dt}\right]\frac{A_n n^2}{A_m n + A_n(N-n)} s\exp\left(-E\Big/kT\right) \tag{28}$$

The peak occurs when the quantity in square brackets is zero,

$$\frac{E\beta}{kT^2} + \left(\frac{2}{n} - \frac{A_m - A_n}{A_m n + A_n(N-n)}\right)\frac{dn}{dt} = 0, \tag{29}$$

$$\frac{E\beta}{kT_m^2} + \left(\frac{2}{n_m} - \frac{A_m - A_n}{A_m n_m + A_n(N-n_m)}\right)\frac{A_m n_m^2}{A_m n_m + A_n(N-n_m)} s\exp\left(-E\Big/kT_m\right) = 0, \tag{30}$$

where n_m is the trap concentration at the maximum and T_m is the temperature at the maximum. Equation (30) is the result of substituting Eq. (24) into Eq. (29). Equation (30) is the maximum condition and provides a relation between β, T_m and n_m. In order to make a variable heating rate plot, we need a second relation between these three variables. This can be found from integrating Eq. (24) over time to find

$$(1 - A_n/A_m)\ln(n_0/n) + \frac{A_n}{A_m}\frac{N}{n_0}\left(\frac{n_0}{n} - 1\right) = \frac{Es}{k\beta}\Gamma(-1, E/kT) - \frac{Es}{k\beta}\Gamma(-1, E/kT_0), \tag{31}$$

where Γ is the incomplete gamma function, $\Gamma(a, x) = \int_x^\infty e^{-x}z^{a-1}dz$. Equation (31) is valid at all times but we will apply it specifically to the maximum. We will assume that the trap is thermally stable at the initial temperature, T_0. Consequently, the second term on the right of Eq. (31) can be neglected. It will be convenient to rewrite Eqs. (30) and (31) as

$$f_1(n_m) = \frac{Es}{k\beta}\left(\frac{kT_m}{E}\right)^2 \exp(-E/kT_m), \tag{32}$$

$$f_2(n_m) = \left(\frac{Es}{k\beta}\right)\Gamma(-1, E/kT_m), \tag{33}$$

where the functions f_1 and f_2 are defined by

$$f_1(n) \equiv \frac{[A_n N + (A_m - A_n)n]^2}{[2A_n N + (A_m - A_n)n]A_m n}, \tag{34}$$

$$f_2(n) \equiv (1 - A_n/A_m)\ln(n_0/n) + \frac{A_n}{A_m}\frac{N}{n_0}\left(\frac{n_0}{n} - 1\right) \tag{35}$$

For any given heating rate β, the corresponding temperature T_m and trap concentration n_m can be obtained by simultaneous solution of Eqs. (32) and (33).

The usual variable heating plot shows β/T_m^2 on a log scale plotted against $1/kT_m$. We can obtain the slope of this curve by taking the log of both sides of Eq. (32) and differentiating with respect to $1/kT_m$. After rearranging, we have

$$\frac{d\ln(\beta/T_m^2)}{d(1/kT_m)} = -E - \left.\frac{d\ln(f_1)}{dn}\right|_{n=n_m}\frac{dn_m}{d(1/kT_m)}. \tag{36}$$

We see that under the general OTOR model, the slope of a variable heating rate plot as given by Eq. (36) will differ from the slope of a simple first-order peak, as given by Eq. (26) by the amount of the second term on the right in Eq. (36). To evaluate the right-hand side of Eq. (36) at a given maximum temperature T_m, we need to know (a) the value of n_m at the peak, (b) the derivative of f_1 and (c) the rate of change of n_m as T_m changes. Since f_1 is an algebraic function of n, Eq. (34), finding the derivative needed for (b) is a simple matter of calculus,

$$\frac{d\ln(f_1)}{dn} = \frac{2(A_m - A_n)}{A_n N + (A_m - A_n)n} - 2\frac{A_n N + (A_m - A_n)n}{[2A_n N + (A_m - A_n)n]n}. \tag{37}$$

To find the information needed for (a) and (c), we start by dividing Eq. (33) by Eq. (32) to obtain

$$\frac{f_2(n_m)}{f_1(n_m)} = G(E/kT_m), \tag{38}$$

where $G(x)$ is defined by

$$G(x) \equiv \frac{\Gamma(-1, x)}{x^{-2}\exp(-x)}. \tag{39}$$

Over the range of interest for thermoluminescence, the function $G(E/kT)$ is, as shown in Fig. 1, a slowly-variable quantity, slightly less than one. Differentiating both sides of Eq. (38) with respect to $1/kT_m$, we have

$$\frac{d(f_2/f_1)}{dn_m}\frac{dn_m}{d(1/kT_m)} = EG'(E/kT_m), \tag{40}$$

where

$$G'(x) = \frac{dG(x)}{dx}. \tag{41}$$

Solving Eq. (40) for $dn/d(1/kT_m)$ and substituting into Eq. (36), we obtain

$$\frac{d\ln(\beta/T_m^2)}{d(1/kT_m)} = -E\left(1 + \frac{d\ln(f_1)/dn}{d(f_2/f_1)/dn}G'(E/kT)\right) \tag{42}$$

Equation (42) details how the slope of a variable-heating-rate plot varies for general one-trap-one-center (OTOR) case. Comparing Eq. (42) with Eq. (27), we see that the correction factor, C_f, for the general OTOR case is

$$C_f = 1 + \frac{d\ln(f_1)/dn}{d(f_2/f_1)/dn}G'(E/kT). \tag{43}$$

Before exploring the general case of OTOR, we will consider the special cases of first- and second-order kinetics, and a third limiting case that is neither of first nor of second order.

4.2. Limiting case: first-order kinetics

Reaction kinetics are described as first order when $dn/dt \propto n$. The one-trap one-center system reduces to first-order kinetics when the recombination coefficient, A_m, is large enough relative to the retrapping coefficient, A_n, and the dose as measured by the trap population, n, is high enough that

$$\frac{A_n}{A_m}\frac{N}{n} << 1. \tag{44}$$

In this case, f_1 (Eq. (34)) and f_2 (Eq. (35)) reduce to

$$f_1(n) = 1, \tag{45}$$

$$f_2(n) = \ln(n_0/n). \tag{46}$$

Combining Eq. (45) and Eq. (46) with Eq. (38), the trap concentration at the maximum can be found,

$$n_m = n_0 \exp[-G(E/kT_m)]. \tag{47}$$

Since, from Fig. 1, G is slightly less than one over the range of interest, Eq. (47) tells us that the trap concentration at the maximum, n_m, is slightly larger than $n_0/e = n_0/2.718$.

Because in first-order kinetics, as per Eq. (45), f_1 is a constant, it follows that $d\ln(f_1)/dn = 0$, and thus the correction factor C_f of Eq. (43) is

$$C_f = 1 \text{ for first-order kinetics} \tag{48}$$

and the slope of the VHR plot is

$$\frac{d\ln(\beta/T_m^2)}{d(1/kT_m)} = -E \text{ for first order kinetics} \tag{49}$$

This is in agreement with prior work (see e.g., Hoogenstraaten, 1958).

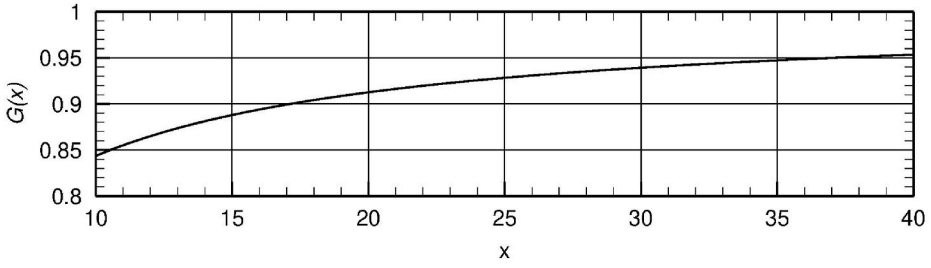

Fig. 1. $G(x)$ as defined by Eq. (39) is plotted against x over the range of interest for thermoluminescence: $10 < x < 40$.

4.3. Limiting case: second-order kinetics

Second-order kinetics is defined by $dn/dt \propto n^2$. From Eq. (24), it is apparent that the OTOR model reduces to second-order kinetics when either $A_m = A_n$ or the dose is low enough that

$$\frac{|A_m - A_n|}{A_n}\frac{n}{N} << 1. \tag{50}$$

In this case, f_1 (Eq. (34)) and f_2 (Eq. (35)) reduce to

$$f_1(n_m) = \frac{A_n}{A_m}\frac{N}{2n_m}, \tag{51}$$

$$f_2(n_m) = \frac{A_n}{A_m}\left[\frac{N}{n_m} - \frac{N}{n_0}\right]. \tag{52}$$

Using Eqs. (51) and (52), Eq. (43) simplifies to

$$C_f = 1 + \frac{n_0}{2n_m}G'(E/kT_m). \quad for \ \sec ond \ \ order \ \ kinetics \tag{53}$$

Combining Eq. (51) and Eq. (52) with Eq. (38), the trap concentration at the maximum can be found,

$$n_m = n_0\left(1 - \frac{G(E/kT_m)}{2}\right). \tag{54}$$

Since, from Fig. 1, G is slightly less than one, Eq. (54) tells us that the trap concentration at the maximum is slightly larger than $n_m/2$ and, from the slope of the plot in Fig. 1, that n_m increases as T_m increases.

Using Eq. (54), Eq. (53) further reduces to

$$C_f = 1 + \frac{G'(E/kT_m)}{2 - G(E/kT_m)}, \quad for \ \sec ond \ \ order \ \ kinetics \tag{55}$$

and the slope on the VHR plot is

$$\frac{d\ln(\beta/T_m^2)}{d(1/kT_m)} = -E\left[1 + \frac{G'(E/kT_m)}{2 - G(E/kT_m)}\right] \quad for \ \sec ond \ \ order \ \ kinetics \tag{56}$$

For second-order kinetics, the correction factor is a function only of E/kT_m and independent of all other trap and center parameters. This quantity, as shown in Fig. 2 is within 1% of one for $E/kT_m > 11$.

The plot in Fig. 1 shows that G is a slowly varying function. Consequently, its derivative G' is small and this is why, from Eq. (55), the correction factor, C_f for second order is close to one.

For second order, it is also possible to obtain the heating rate β explicitly as a function of the peak temperature. To do this, we combine Eq. (30) and Eq. (51) with Eq. (32). After rearranging, we find

$$\beta = \frac{Es}{k}\frac{A_m}{A_n}\frac{n_0}{N}[2 - G(E/kT_m)]\exp(-E/kT_m). \tag{57}$$

Sample calculations are shown in Fig. 3 comparing the general OTOR model with the second-order limit as given by Eq. (56). The second-order approximation is shown to be accurate when the conditions in Eq. (50) are obeyed.

4.4. Limiting case: high-dose and strong retrapping

With weak retrapping, Eq. (44) and at any dose level, the governing equation for OTOR, Eq. (24) reduces to first-order kinetics, with $dn/dt \propto n$. With strong retrapping and low dose, as in Eq. (50), then Eq. (28) reduces to second-order kinetics with $dn/dt \propto n^2$. There is a third case characterized by strong retrapping and high dose,

$$A_n/A_m >> 1 \quad and \quad n \sim N. \tag{58}$$

In this case, Eq. (24) reduces to

$$I = -\frac{dn}{dt} = \frac{n^2}{N-n}\frac{A_m}{A_n}s\exp(-E/kT). \tag{59}$$

Neither first- nor second-order applies. While we can still obtain the exact solutions for this case using the methods of Sec 4.1, it is useful to develop approximate solutions that show the magnitudes and scaling factors in this case. For the case of strong retrapping and possibly high dose, Eq. (59), the formulas for f_1 and f_2, Eqs. (34) and (35), respectively, reduce to

$$f_1(n) = \frac{A_n}{A_m}\frac{(N-n)^2}{(2N-n)n}, \tag{60}$$

$$f_2(n) = \frac{A_n}{A_m}\left[\frac{N}{n} - \frac{N}{n_0} - \ln(n_0/n)\right]. \tag{61}$$

Using Eq. (60) and Eq. (61) Eq. (38) reduces to

$$\frac{(2N-n_m)N}{(N-n_m)^2}\left[1 - \frac{n_m}{n_0} - \frac{n_m}{N}ln(n_0/n_m)\right] = G(E/kT_m). \tag{62}$$

The key point to notice about Eq. (62) is that the rate constants A_n and A_m do not appear in it. This means that for a given value of E/kT_m and a given relative dose n_0/N, Eq. (62) determines the relative trap concentration at the maximum, n_m/n_0. With this information, Eqs. (60) and (61) can be combined with Eq. (43) where A_n and A_m again cancel out, to determine the correction factor C_f for the variable heating plot. This allows the creation of the plot shown in Fig. 4. It can be seen that the correction factor C_f is largest when the trap is initially saturated, $n_0 = N$, and the E/kT_m is lowest. As the dose declines, the correction factor C_f approaches that of the second-order theory, Eq. (55). This can be verified by noting that Eq. (62) reduces to Eq. (54) in the low-dose limit, $n_0/N \to 0$.

In Fig. 5, results for high dose, $n_0/N = 1$, from the strong trapping high-dose model (dashed lines) are compared with the exact OTOR solution (solid lines) for $\beta = 1$, $E = 1$eV, and two different values of s as shown.

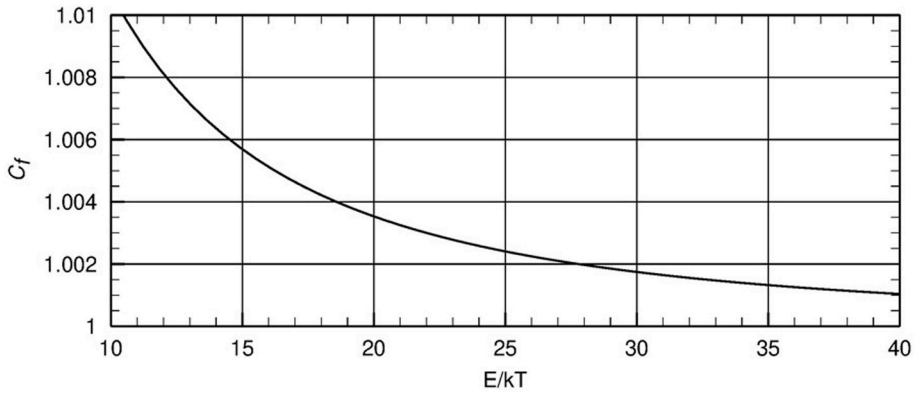

Fig. 2. The correction factor C_f for the slope of a variable heating rate plot for second-order kinetics (Eq. (55)) is plotted against E/kT_m.

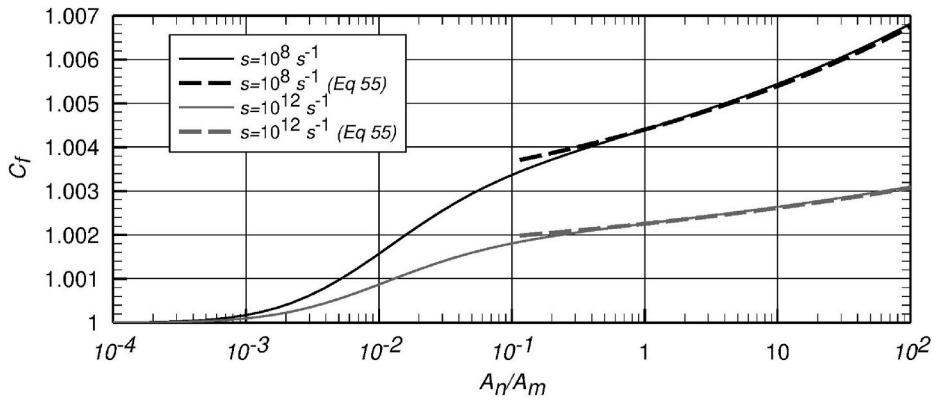

Fig. 3. The variable-heating-rate correction factor, C_f, is shown for the OTOR model. The calculation assumes $\beta = 1$ K/s, $E = 1$ eV and $n_0/N = 0.01$. The values of s and A_n/A_m are as shown. The solid lines are the exact result for OTOR. The dashed lines assume second-order kinetics.

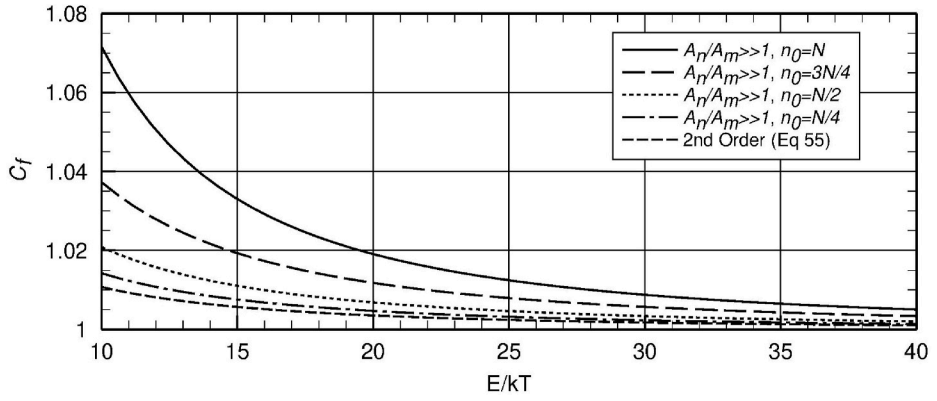

Fig. 4. The correction factor C_f for variable heating rate plot is shown as a function of E/kT_m for the strong-retrapping limit at four levels of the dose n_0/N. Also shown for comparison is the case of second-order kinetics. The highest correction factors occur for strong retrapping at high dose, and low values of E/kT_m.

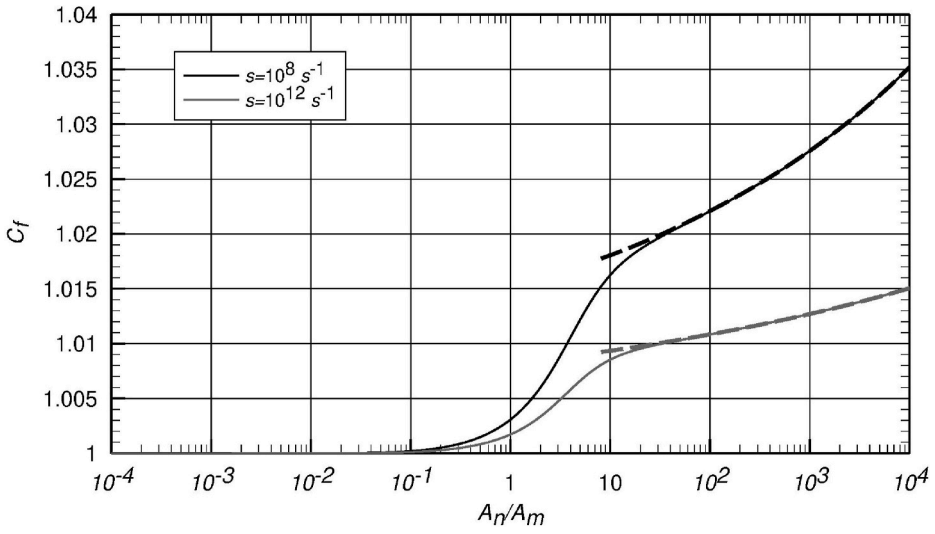

Fig. 5. The variable-heating-rate correction factor, C_f, is shown for the OTOR model for high dose, $n_0/N = 1$. The other conditions are the same as in Fig. 3. The solid lines are the exact result for OTOR. The dashed lines assume strong-retrapping and high dose. For strong retrapping, these results produce a larger correction factor than the low-dose results of Fig. 3. For weak retrapping, $A_n/A_m << 1$, the correction factor at high dose is seen to be much closer to one than the corresponding results at low dose in Fig. 3.

4.5. Summary of the general analytical approach

To interpret the slope of a variable heating-rate plot, we have identified three special cases:

- Case 1: For first-order kinetics, Eq. (44), the correction factor is $C_f = 1$ and the slope on the VHR plot is the same as the trap energy, E.
- Case 2: For second-order kinetics, Eq. (50), the correction factor is typically close to one: $1 \le C_f \le 1.01$. To correct for this factor, one can start by dividing the slope on the plot by kT_m to obtain a first estimate for E/kT_m and, using this value, compute the correction factor from Eq. (55) or read it off from the plot in Fig. 2. The slope of the VHR plot is divided by C_f to obtain the better estimate of trap energy E.

- Case 3: For the case of strong retrapping and high dose, Eq. (58), larger correction factors are possible. If this case applies, the slope on the VHR plot will be observed to depend on dose as dose approaches saturation. This effect will be significant if the peak occurs at lower values of E/kT_m as shown in Fig. 4. One approach for estimating the trap energy in this case is to use a dose high enough to reach saturation, $n_0 = N$, and then read the correction factor C_f from the top curve in Fig. 4. Alternatively, one can use the low dose in which case the correction factor can be estimated from the second-order curve in Fig. 4 or Fig. 2.

5. Applying the VHR method and the Maghrabi equations for mixed-order kinetics (MOK)

The mixed-order kinetics has been considered as a possible process governing thermoluminescence. As presented by Chen et al. (1981), the governing equation is

$$I(T) = -dn/dt = s' n^2 \exp(-E/kT) + s' Cn \exp(-E/kT), \quad (63)$$

where s' is a constant with units of $cm^3 s^{-1}$, and C has units of concentration, cm^{-3}. Equation (6) in Kitis and Gómez-Ros (1999) showed that in the MOK model, the condition for the maximum temperature T_m in a TL glow curve becomes

$$\frac{\beta E}{kT_m^2 R_m} = Cs' \exp(-E/kT_m) \quad (64)$$

where R_m is a dimensionless constant.

Kitis and Gómez-Ros (1999) evaluated the parameter R_m in a very broad range of the trapping parameters $E = 0.6$–2.2 eV, $s' = 10^7$-$10^{22} s^{-1}$ and the mixed-order kinetic parameter $\alpha = 0.1$–0.95 where $\alpha = n_0/(n_0 + C)$ and n_0 is the initial value of n. These authors found that within this broad range of values, the parameter R_m depends only on the mixed-order-kinetics parameter α, according to the following approximate empirical equation (their Eq. (17)),

$$R_m(\alpha) = \frac{2.6 - 0.9203\alpha + 0.324\alpha^{3.338}}{2.6 - 2.9203 + 0.324\alpha^{3.338}}. \quad (65)$$

By combining the previous two equations we obtain

$$\frac{\beta E}{kT_m^2} = Cs' R_m(\alpha) \exp(-E/kT_m), \quad (66)$$

$$\frac{\beta E}{kT_m^2} = s'' \exp(-E/kT_m), \quad (67)$$

where s'' is a constant with dimensions of frequency (s^{-1}), which does not depend on the heating rate used during the experiment.

This equation has the exact same form as Eq. (3), with the only difference being the effective constant frequency factor $s'' = Cs' R_m(\alpha)$ replacing the frequency factor s. Therefore, both the VHR method and the Maghrabi equation are applicable to the MOK model.

6. Applying the VHR method and the Maghrabi equation to feldspars

Jain et al. (2012) developed a localized transitions model for feldspars, which has been used extensively to quantify luminescence signals in these materials. This model is based on quantum tunneling processes taking place in random distribution of defects in a crystal.

Kitis and Pagonis (2014) carried out a detailed simulation study of the properties of TL glow curves in this model, by varying randomly the parameters in the model within a wide range of physically possible values. They obtained the following general expression in their Eq. (21)

$$\frac{\beta E}{kT_m^2} = f_m(\rho') sz \exp(-E/kT_m) \quad (68)$$

where f_m is a dimensionless quantity, ρ' is the dimensionless acceptor density parameter characterizing the material and z = 1.8 is a constant in the model. Kitis and Pagonis (2014) further showed that the dimensionless quantity f_m depends only on the acceptor density parameter ρ', according to the following empirical equation which is derived from the simulation data in their Fig. 5b,

$$f_m(\rho') = 4.90537(\rho')^{1.21038}. \quad (69)$$

By combining the two previous equations, one gets

$$\frac{\beta E}{kT_m^2} = s_{eff} \exp(-E/kT_m) \quad (70)$$

where $s_{eff} = f_m(\rho')sz$ is a constant with dimensions of frequency (s^{-1}), which once more does not depend on the heating rate used in the experiment. This equation has again the exact same form as Eq. (3) and therefore, both the VHR method and the Maghrabi equation are applicable for this feldspar model.

7. Discussion

In the present work, we have considered some points related to the method of various heating rates for the evaluation of the activation energy of traps from TL curves by monitoring the shift of the maximum due to a change in the heating rate. For the behavior of first-order peaks, we have shown that an explicit expression, Eq. (8), previously presented by Maghrabi (2018) as a heuristic expression, can be developed analytically with very reasonable approximations. Also, a more precise expression, Eq. (18), is presented which is slightly better though somewhat more complicated.

The other point has to do with the generality of the various heating rates method. We have solved numerically the set of three simultaneous differential equations governing the process in the OTOR system of one trapping state and one kind of recombination center with two heating rates. Keeping all the parameters fixed and varying only the retrapping probability coefficient, we see the gradual transition from first to second order kinetics, including intermediate cases in the sense that the symmetry factor is between 0.42 and 0.52, values associated with first and second order kinetics, respectively. Although the method shown in Eq. (5) (and its extension to several heating rates; see comment following Eq. (5)) was directly developed for first-order peaks, it seems that the method is useable for more complex situations as shown here. The results in Table 1 are, of course, only an example with accuracy of determining E better than 0.25%. An analytical analysis over the full range of parameters for the OTOR model similarly shows that Eq. (5) typically remains quite accurate. If one wants to improve the accuracy, the analytical method for determining a correction factor was developed. For the case of second-order kinetics, the correction factor depends only on E/kT_m and is given by Eq. (55) (Fig. 2). The largest difference between Eq. (5) and the OTOR model, as much as 7%, occurs for the special case of strong retrapping combined with very high dose. To refrain from this situation, one should use smaller doses, farther from saturation dose. The correction factors for this case, as shown in Fig. 4, depend on the dose. The general applicability of Eq. (5) appears to extend to the more complex situation where the glow curve includes a number of peaks. This is so in particular since it has been shown that in the case of a number of peaks in a series, the individual peaks tend to behave like first-order curves, excluding the last peak in the series which tends to be of second order; see e.g. Chen and Pagonis (2013). We have also dealt with the various heating rates behavior of TL peaks governed by the "mixed order" kinetics and showed that the variable-heating-rate method applies here as well.

Finally, this work has dealt only with the theoretical aspects of the different heating rates method. In practice, one should remember that there is usually some delay between the temperature of the heating plate and the TL sample, and the size of the delay increases with the heating

rate. A possible correction for the temperature lag has been offered by Kitis and Tuyn (1998) so as to get more reliable results by the VHR method.

Declaration of competing interest

The authors declare that they have no known competing financial interests or personal relationships that could have appeared to influence the work reported in this paper.

References

Bohun, A., 1954. Thermoemission und photoemission von natriumchlorid. Czech. J. Phys. 4, 91–93.
Booth, A.H., 1954. Calculation of electron trap depths from thermoluminescence maxima. Can. J. Chem. 32, 214–216.
Chen, R., Winer, S.A.A., 1970. Effects of various heating rates on glow curves. J. Appl. Phys. 41 (13), 5227–5232.
Chen, R., Kristianpoller, N., Davidson, Z., 1981. Mixed first and second order kinetics in thermally stimulated processes. J. Lumin. 23, 293–303.
Chen, R., Pagonis, V., 2013. On the expected order of kinetics in a series of thermoluminescence (TL) and thermally stimulated conductivity (TSC) peaks. NIMB 312, 60–69.
Garlick, G.F.J., Gibson, A.F., 1948. The electron-trap mechanism of luminescence in sulphide and silicate phosphors. Proc. Phys. Soc. 60, 574–590.
Halperin, A., Braner, A.A., 1960. Evaluation of thermal activation energies from glow curves. Phys. Rev. 117, 408–415.
Hoogenstraaten, W., 1958. Electron traps in zinc-sulphide phosphors. Philips Res. Rep. 13, 515–693.
Jain, M., Guralnik, B., Anderson, M.T., 2012. Stimulated luminescence emission from localized recombination in randomly distributed defects. J. Phys. Condens. Matter 24 (38), 385402.
Kannunikov, I.A., 1978. Reaction order of thermally stimulated recombination. J. Appl. Spectrosc. 28, 597–599.
Kitis, G., Gómez-Ros, J.M., 1999. Glow corve deconvolution functions for mixed-order kinetics and a continuous trap distribution. Nucl. Instrum. Methods A 440, 224–231.
Kitis, G., Pagonis, V., 2014. Properties of thermoluminescence glow curves from tunneling recombination processes in random distributions of defects. J. Lumin. 153, 118–124.
Kitis, G., Tuyn, J.W.N., 1998. A simple method to correct for the temperature lag in TL glow-curve measurements. J. Phys. D Appl. Phys. 21, 2065–2073.
Maghrabi, M., 2018. Dependence of the peak shift, peak height and FWHM of thermoluminescence peaks on the heating rate and trap parameters. J. Lumin. 198, 54–58.
May, C.E., Partridge, J.A., 1964. Thermoluminescent kinetics of alpha-irradiated alkali halides. J. Chem. Phys. 40, 1401–1409.
Osada, K., 1960. Thermoluminescence of zink sulfide phosphors. J. Phys. Soc. Japan 15, 145–149.
Parfianovitch, I.A., 1954. The determination of trap depth of electron traps in crystal phosphors. J. Exp. Theor. Phys. USSR 26, 696–699.
Randall, J.T., Wilkins, M.H.F., 1945. Phosphorescence and electron traps I. The study of trap distributions. Proc. Roy. Soc. A184, 347–390.